Oligomers of the Cytoplasmic Fragment from the *Escherichia coli* Aspartate Receptor Dissociate through an Unfolded Transition State†

Stacy K. Seeley,‡ Günther K. Wittrock,§ Lynmarie K. Thompson,*,‡,§ and Robert M. Weis*,‡,§

Department of Chemistry and Graduate Program in Molecular and Cellular Biology, University of Massachusetts, Amherst, Massachusetts 01003

Received July 16, 1996⊗

ABSTRACT: The kinetic and equilibrium properties of a clustering process were studied as a function of temperature for two point mutants of a 31 kDa fragment derived from the cytoplasmic region of the *Escherichia coli* aspartate receptor (C-fragment), which were shown previously to have a greater tendency to form clusters relative to the wild-type C-fragment [Long, D. G., & Weis, R. M. (1992) *Biochemistry 31*, 9904−9911]. The clustering equilibria were different for the two C-fragments. Monomers of a serine-461 to leucine (S461L) mutant C-fragment were in equilibrium with dimers, while monomers of a S325L C-fragment were in equilibrium with trimers. The positive values for $\Delta H°$, $\Delta S°$, and $\Delta C_p°$ of dissociation estimated from a van't Hoff analysis, and the differences in the CD spectra of isolated monomers and oligomers, demonstrated that the monomers were less well-folded than the clustered forms. The oligomer dissociation rate exhibited a marked temperature dependence over the range from 4 to 30 °C and was remarkably slow at low temperatures; e.g. $t_{1/2}$ of dimer dissociation for the S461L C-fragment was 85 h at 4 °C. The values for $\Delta H°^{‡}$, $\Delta S°^{‡}$, and $\Delta C_p°^{‡}$ derived from the temperature dependence of the dissociation rate were comparable to the corresponding parameters determined in a DSC study of C-fragment denaturation [Wu, J., Long, D. G., & Weis, R. M. (1995) *Biochemistry 34*, 3056−3065], which indicated that the transition state resembled thermally denatured C-fragment. Octyl glucoside accelerated the dissociation rate by 3−5-fold presumably by lowering the barrier to dissociation. This acceleration and the positive value of $\Delta C_p°^{‡}$ were interpreted as evidence for an increase in solvent accessible hydrophobic groups in the transition state. The molecular basis for the slow rate of dissociation is proposed to result from the conversion of intermolecular coiled coils in the oligomers to an intramolecular coiled coil in the monomer.

The aspartate, serine, ribose/galactose, and dipeptide receptors in the chemosensory system of *Escherichia coli* comprise a homologous family of integral membrane proteins which bind specific ligands and initiate a signal transduction pathway that biases cell motility [for recent reviews, see Hazelbauer et al. (1993), Parkinson (1993), and Blair (1995)]. The members of this family share the same membrane topology: a periplasmic ligand-binding domain, two α-helical membrane-spanning segments, and a cytoplasmic domain that is coupled to the phosphorylation cascade through interactions with the kinase CheA. The X-ray crystal structure of the ligand-binding domain (Milburn et al., 1991; Yeh et al., 1993; Bowie et al., 1995) and the site-directed disulfide cross-linking studies of the transmembrane segments (Pakula & Simon, 1992; Lee et al., 1994) have provided evidence for the dimeric arrangement of receptor subunits in the membrane. Although detailed structure data are not yet available for the cytoplasmic domain, sequence-based analyses predict significant regions of α-helical coiled coils (Stock et al., 1991; Cochran & Kim, 1996). Within these coiled-coil segments are found the glutamic acid residues which are reversibly methylated during the adaptation process, such that the suppression of kinase activity caused by attractant binding is reversed by an increase in the level of methylation.

Point mutations have been generated by chemical mutagenesis of the aspartate and serine receptors which were localized in the cytoplasmic region and resulted in biased swimming behavior in the cell toward either of two extremes, constant tumbling or smooth swimming (Mutoh et al., 1986; Ames & Parkinson, 1988). Since these behavioral extremes are correlated with two extremes in receptor signaling, kinase activation and inhibition, respectively (Borkovich & Simon, 1991), the mutations can be regarded as locking the receptor into either one of two signaling states. The mutations exerted their effect independent of the ligand-binding and transmembrane domains since cytoplasmic fragments derived from the aspartate receptor were observed to produce some of the same effects on signaling *in vivo* (Oosawa et al., 1988), and similar "locked" C-fragments from the *E. coli* serine receptor modulated CheA activity in the expected manner (Ames & Parkinson, 1994; Ames et al., 1996). The observed

† This research was supported by U.S. Public Health Service Grants GM47601 (L.K.T.) and GM42636 (R.M.W.), an award from Research Corp. (L.K.T.), an NSF Young Investigator Award (L.K.T.), and a Beckman Young Investigator Award (R.M.W.).

* To whom corrrespondence should be addressed: R.M.W. [Phone: (413) 545-0464. E-mail: rmweis@chem.umass.edu. Fax: (413) 545-4490.] and L.K.T. [Phone: (413) 545-0827. E-mail: thompson@chem.umass.edu.].

‡ Department of Chemistry.

§ Graduate Program in Molecular and Cellular Biology.

⊗ Abstract published in *Advance ACS Abstracts,* November 15, 1996.

[1] Abbreviations: CD, circular dichroism; GFC, gel filtration chromatography; OG, octyl β-D-glucopyranoside; C-fragment, 257−553 amino acid residue fragment of the *Escherichia coli* aspartate receptor; CMC, critical micelle concentration.

S0006-2960(96)01749-7 CCC: $12.00

correlation between the smooth swimming bias induced by the "smooth" mutations in the intact receptor and the pronounced tendency for the C-fragment proteins containing these mutations to cluster in solution (Long & Weis, 1992) suggested that the clustering process may play a role in signaling and has thus prompted further study of the clustering equilibrium.

The association−dissociation kinetics of two oligomer-forming C-fragments, S461L and S325L, have been studied by GFC and CD as a function of temperature (4−30 °C). The interconversion between oligomer and monomer was observed to be extremely slow at the lower end of this range. The analysis of the rate data by absolute rate theory indicates that the C-fragment oligomers must unfold before dissociating. Also, the analysis of the data obtained at equilibrium suggested that the monomeric C-fragments were not as well folded as the oligomers. From these data, a model is proposed for the dissociation process in which the intermolecular coiled coils of the oligomers separate and form intramolecular coiled coils in the dissociated monomers.

MATERIALS AND METHODS

Chemicals, Plasmids, and Bacterial Strains. OG was obtained from Calbiochem (La Jolla, CA). DEAE-Sepharose CL-6B was purchased from Sigma Chemical Co. (St. Louis, MO). Isopropyl β-D-galactoside was obtained from Bachem (Torrance, CA), and Affi-Gel Blue Gel was purchased from Bio-Rad Laboratories (Melville, NY). All chemicals were reagent grade. JM103 [*sup*E *thi*- Δ(*lac-pro*AB), F′[*tra*D36 *pro*AB *lac*I^q]] was the *E. coli* host used for pNC189, the C-fragment expression plasmid which encodes the 297-amino acid C-terminal fragment of the wild-type aspartate receptor from *E. coli* (Kaplan & Simon, 1988). Derivatives of pNC189 were used to produce C-fragments with serine to leucine mutations at position 325 and 461 (Long & Weis, 1992) in which the residue number refers to the position in the intact receptor (553 amino acids).

Bacterial Growth and C-Fragment Purification. C-fragment purification was carried out as described by Long and Weis (1992) with an additional analytical GFC purification step in which 100 μL aliquots were injected onto a TSK-gel G3000SW$_{XL}$ GFC column (The NEST Group, Southborough, MA) and oligomer and monomer fractions were collected and concentrated in an Amicon G-10 ultrafilter (Amicon, Beverly, MA). C-fragment concentrations were determined by absorbance at 280 nm using an ϵ_{280} value of 7500 M^{-1} cm^{-1} (Long & Weis, 1992). Sodium phosphate buffer (pH 7.0, 20 mM) containing 50 mM NaCl and 1 mM EDTA was used in all the experiments described here.

Analytical Gel Filtration Chromatography. A TSK-gel G3000SW$_{XL}$ GFC column was used to separate oligomers and monomers, as described previously (Long & Weis, 1992). Relative concentrations were determined using a Rainin UVC variable-wavelength detector tuned to either 280 or 214 nm. The GFC column was calibrated with the globular molecular mass standards (kilodaltons): β-amylase (200), alcohol dehydrogenase (150), transferrin (78), ovalbumin (45), carbonic anhydrase (29), and cytochrome *c* (12.4).

Determination of the Oligomerization State by Static Light Scattering. A mini-DAWN multiangle static light-scattering instrument (Wyatt Technology Corp., Santa Barbara, CA) and a Rainin UVC absorbance detector were used in sequence to determine the concentration-normalized scattering power at 690 nm of the GFC fractions at 4 °C. Using the known molecular mass of the monomer form of the C-fragment, the weight-average molecular masses for the oligomer peaks ($M_{W,n}$) of S461L and S325L C-fragment proteins were calculated using eq 1

$$M_{W,n} = M_{W,m}\frac{(I_n/C_n)}{(I_m/C_m)} \quad (1)$$

in which the molecular mass of the oligomer is equal to the molecular mass of the monomeric C-fragment ($M_{W,m}$) multiplied by the ratio of the intensities of excess scattered light for the oligomeric and monomeric forms, I_n/C_n and I_m/C_m, respectively, which are normalized according to mass concentrations (Dollinger et al., 1992). The estimates of the molecular mass (in Figure 1) were calculated using a refractive index for the buffer of 1.331 (Angelides et al., 1979), and a value of 0.2 cm^3/g was used for d*n*/d*c* of the C-fragment (Long & Weis, 1992). The uncertainties reported for the molecular mass ratios were estimated by error propagation from the uncertainty in the fits of light scattering data.

Determination of the Oligomerization State by Gel Filtration Chromatography. A stock solution of the S325L C-fragment was serially diluted to make samples over the concentration range from 12 to 94 μM and were allowed to reach equilibrium over a period of 1 week at 4 °C. Samples were then analyzed by GFC (as described above), and the fractions of monomer and oligomer were determined using peak heights. From the expression for the equilibrium dissociation constant (K_d), a linear relationship between the monomer concentration (f_mM_{tot}) and the concentration of monomer as oligomer (f_nM_{tot}) was obtained

$$\log(f_nM_{tot}) = n\log(f_mM_{tot}) - \log(K_d/n) \quad (2)$$

in which the slope of the plot of $\log(f_nM_{tot})$ as a function of $\log(f_mM_{tot})$ was used to determine the reaction molecularity (n).

Kinetics of Dissociation Using Gel Filtration Chromatography. A 100 μL injection of initial stock C-fragment protein (1.5−3.0 mg/mL) was injected onto the GFC column, and the diluted oligomer fraction (ca. 1.5 mL) was collected. Each of these collected oligomer samples was incubated in a precision water bath (Neslab RTE-211, Neslab Instruments, Inc., Newington, NH) at various temperatures (4.0, 9.0, 14.0, 18.0, 23.0, 27.0, and 30.0 °C). The re-equilibration between oligomer and monomer was followed by injecting 100 μL aliquots of the isolated oligomer fraction at various times and analyzing the areas of the absorbance peaks with Rainin Dynamax software. For each time point, the oligomer fraction was calculated by dividing the area of the oligomer peak by the sum of the areas for oligomer and monomer. Rate data at a particular temperature were typically collected from several samples of the oligomer fraction derived from the stock solution; oligomer concentrations of all these collected oligomer samples were determined by UV absorbance, and the averaged value was used as the protein concentration for the pooled data. The reproducibility in the concentration of collected oligomer was quite good; the variation from one sample to the next was less than 10%.

Table 1: Rate Data for the Dissociation of S461L C-Fragment Dimers[a]

no.	protein concentration[b] (μM)	method	T (°C)	$f_{d,eq}$	K_d (μM)	$k_d \times 10^6$ (s^{-1})	k_a (M^{-1} s^{-1})
1	2.9	GFC	4.0	0.53 ± 0.01	2.4 ± 0.3	2.3 ± 0.2	0.9 ± 0.1
2	4.2	GFC	9.0	0.48 ± 0.05	4.7 ± 0.5	3.6 ± 0.6	0.7 ± 0.1
3	4.0	GFC	14.0	0.43 ± 0.01	6.0	7.8 ± 0.7	1.3
4	1.9	GFC	18.0	0.34 ± 0.01	4.9	19 ± 2	4.0
5	3.4	GFC	23.0	0.32 ± 0.01	9.8	44 ± 3	4.3
6	7.9	CD	23.0	0.46 ± 0.01	10	85 ± 5	8.3
7	3.1	GFC	27.0	0.26 ± 0.01	13	153 ± 10	12
8	3.1	GFC	30.0	0.22 ± 0.01	17	328 ± 17	17
9	6.0	CD	30.0	0.28 ± 0.01	22	488 ± 17	22

[a] Uncertainties in $f_{n,eq}$ and k_d are standard errors determined from the curve-fitting routine. The stated uncertainties in k_a and K_d were determined by the propagation of error from the uncertainty estimates of $f_{n,eq}$ and k_d; otherwise, errors of 10% were assumed for k_a and K_d on the basis of the uncertainty in the total C-fragment concentration (M_{tot}). [b] Protein concentrations are expressed in moles of monomer.

Table 2: Rate Data for the Dissociation of S325L C-Fragment Trimers[a]

no.	protein concentration[b] (μM)	method	T (°C)	$f_{t,eq}$	K_d (μM)^2	$k_d \times 10^6$ (s^{-1})	$k_{app} \times 10^{-6}$ (M^{-2} s^{-1})
10	1.5	GFC	4.0	0.13 ± 0.01	34	53 ± 8	1.6 ± 0.4
11	2.9	GFC	9.0	0.24 ± 0.01	46	42 ± 6	0.9 ± 0.4
12	3.2	GFC	14.0	0.27 ± 0.01	44	51 ± 6	1.2 ± 0.5
13	1.7	GFC	18.0	0.16 ± 0.01	32	78 ± 11	2.4 ± 0.2
14	2.7	GFC	23.0	0.15 ± 0.01	90	149 ± 15	1.7 ± 0.5
15	2.4	CD	23.0	0.14 ± 0.01	78	183 ± 15	2.3 ± 0.5
16	8.0	GFC	27.0	0.26 ± 0.01	300	282 ± 15	1.0 ± 0.4
17	10.7	GFC	30.0	0.25 ± 0.01	580	564 ± 38	1. 0 ± 0.4
18	3.3	CD	30.0	0.06 ± 0.01	450	703 ± 31	1.7 ± 0.3

[a] Uncertainties in $f_{n,eq}$ and k_d are standard errors determined from the curve-fitting routine. The stated uncertainties in k_{app} were determined by the propagation of error from the uncertainty estimates of $f_{n,eq}$ and k_d. Errors of 10% were assumed for K_d on the basis of the uncertainty in the total C-fragment concentration (M_{tot}). [b] Protein concentrations are expressed in moles of monomer.

For experiments probing the effect of detergent on C-fragment dissociation, 0.25% (w/v) OG was added to the oligomer sample immediately before it was placed in the temperature-regulated water bath.

The kinetic data for the S461L smooth mutant were fit to the analytic expression of the integrated rate equation for dissociation of a dimer:

$$f_d = \frac{f_{d,0} - f_{d,eq} + f_{d,eq}(1 - f_{d,0} f_{d,eq}) \exp\left(\frac{1 + f_{d,eq}}{1 - f_{d,eq}} k_d t\right)}{f_{d,eq}(f_{d,0} - f_{d,eq}) + (1 - f_{d,0} f_{d,eq}) \exp\left(\frac{1 + f_{d,eq}}{1 - f_{d,eq}} k_d t\right)} \quad (3)$$

where $f_{d,0}$, f_d, and $f_{d,eq}$ are the dimer fractions at the beginning of the experiment ($t = 0$), at time t, and at equilibrium ($t \rightarrow \infty$), respectively, and k_d is the dissociation rate constant (see the Appendix). In the fitting of the experimental data (f_d *versus* t) to eq 3, $f_{d,0}$, $f_{d,eq}$, and k_d were adjustable, which were then used with the total concentration of C-fragment to calculate the equilibrium dissociation constant K_d and the association rate constant k_a. The equilibrium for the S325L C-fragment was best described as a monomer−trimer process; fits to the data were obtained by iterative numerical integration of the corresponding rate equation for the trimer dissociation using a fourth-order Runge−Kutta algorithm (Press et al., 1986). The uncertainties in k_d and $f_{n,eq}$ reported in Tables 1 and Table 2 are standard errors of these parameters derived from the χ^2 value of the fit. The relative uncertainties in K_d and k_a were assumed to be equivalent to the relative uncertainty in the protein concentration (*ca.* 10%), since this was in most cases substantially greater than the standard errors derived from χ^2.

Temperature Dependence of the Clustering Equilibria. The temperature dependence of $\Delta G°$ of oligomer dissociation (obtained from kinetic data via $\Delta G° = -RT \ln K_d$) was analyzed in plots of $\Delta G°$ (kilocalories per mole) *versus* temperature (kelvin). The nonlinearity of the data required the use of a form of $\Delta G°$ which accounted for the temperature dependence of $\Delta H°$ and $\Delta S°$:

$$\Delta G° = \Delta H° + \Delta C_p°(T - T_r) - T\left[\Delta S° + \ln\left(\frac{T}{T_r}\right)\right] \quad (4)$$

in which the change in heat capacity accompanying dissociation, $\Delta C_p°$, was assumed to be temperature-independent and $\Delta H°$ and $\Delta S°$ were the changes in enthalpy and entropy at the reference temperature T_r (298 K), respectively.

Temperature Dependence of Dissociation Rates. Eyring plots [$\ln(k_d/T)$ *versus* $1/T$] were made of the rate data

$$\ln\left(\frac{k_d}{T}\right) = \ln\left(\frac{k_B}{h}\right) - \frac{\Delta G°^{‡}}{RT} \quad (5)$$

in which k_B, h, and R are the Boltzmann, Planck, and gas constants, respectively, and $\Delta G°^{‡}$ is the free energy of activation (Glasstone et al., 1941). To account for the nonlinearity in the data, $\Delta G°^{‡}$ was assumed to have a form analogous to $\Delta G°$ in eq 4 in which the temperature dependence of $\Delta H°^{‡}$ and $\Delta S°^{‡}$ was attributed to a non-zero, temperature-independent value of $\Delta C_p°^{‡}$.

Circular Dichroism. Samples enriched in the oligomer and monomer forms of the C-fragments were collected by

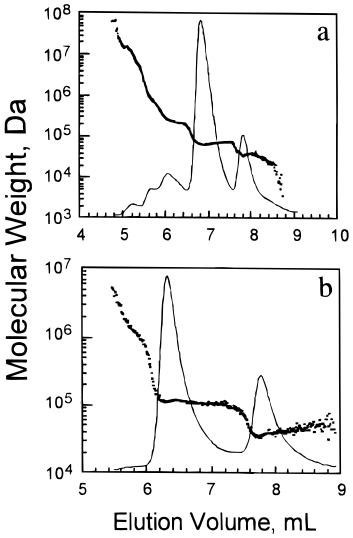

FIGURE 1: Static light scattering of oligomer-forming C-fragments. The absorbance at 280 nm of the GFC chromatograms is overlaid with the weight-averaged molecular masses determined on-line by static light scattering for the (a) S461L smooth mutant C-fragment and the (b) S325L smooth mutant C-fragment.

GFC, and CD spectra of each sample were recorded on an Aviv 62DS circular dichroism spectrometer with thermostatically controlled cell holders as described previously (Wu et al., 1995; Seeley et al., 1996). Ellipticity data at 222 nm were collected from 4 to 84 °C in 2 °C intervals. A 1 mm path length cell, a bandwidth of 1 nm, an equilibration time of 1 min, and an averaging time of 10 s were used. All spectra were processed by subtracting buffer scans. The fractions of monomer and oligomer were determined by GFC before and after the CD spectra were acquired. Protein concentrations were between 0.1 and 0.4 mg/mL.

The CD spectrometer was also used to acquire rate data at 23.0 and 30.0 °C by monitoring the ellipticity at 222 nm. Data were collected every 2 min with a 10 s averaging time over 4 h with a bandwidth of 1 nm in a 1 mm path length cell. Sample concentrations ranged from 0.15 to 0.30 mg/mL; the oligomerization state was analyzed by GFC both before and after the experiment. To compare the CD and GFC kinetic data, ellipticities were converted into the fraction of oligomer (f_n). The ellipticities of samples recorded at the beginning (θ_1) and the end (θ_2) of a kinetics experiment were used with estimates for the fraction of monomer (f_{m1} and f_{m2}) and oligomer (f_{n1} and f_{n2}) obtained by GFC before and after the experiment to determine the ellipticities at 222 nm of oligomer (θ_n) and monomer (θ_m):

$$\theta_n = \frac{f_{m2}\theta_1 - f_{m1}\theta_2}{f_{m2} f_{n1} - f_{m1} f_{n2}} \quad (6)$$

$$\theta_m = \frac{f_{n2}\theta_1 - f_{n1}\theta_2}{f_{n2} f_{m1} - f_{n1} f_{m2}} \quad (7)$$

The fraction of oligomer was then calculated by substituting these values into eq 8:

$$f_n(t) = \frac{\theta(t) - \theta_m}{\theta_n - \theta_m} \quad (8)$$

in which $\theta(t)$ is the ellipticity (at 222 nm) of the sample at time t. Plots of f_n *versus* time were made and analyzed as described above to determine the kinetic constants.

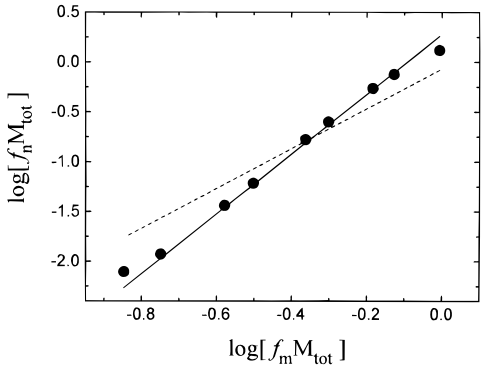

FIGURE 2: Equilibrium distribution of the monomer and oligomer form of the S325L smooth mutant C-fragment at various concentrations: experimental data (●), the line for monomer−trimer equilibrium (—), and the line for monomer−dimer equilibrium (---).

RESULTS

The S325L C-Fragment Is Involved in a Monomer−Trimer Equilibrium. The monomer and oligomer forms of the two C-fragments were separated by GFC. As shown in Figure 1, the UV absorbance profile indicated that the S461L C-fragment eluted mainly in two peaks with apparent molecular masses of 110 and 220 kDa (calibrated against globular protein standards) and that the S325L smooth mutant C-fragment eluted in two peaks of 110 and 270 kDa (Figure 1), in agreement with the previous observations of Long and Weis (1992). Batch-mode static light scattering experiments have demonstrated that the 110 kDa form identified by GFC corresponded to the 31 kDa monomer and that the 220 kDa form of the S461L C-fragment corresponded to a dimer (Long & Weis, 1992).

On-line static light scattering was used to determine the oligomerization state of the S325L C-fragment and to confirm the dimeric state of the S461L C-fragment as they eluted from the GFC column. In the GFC traces of Figure 1, protein absorbance traces are overlaid with the corresponding weight-averaged molecular masses estimated by light scattering. From the light scattering data, oligomer to monomer molecular mass ratios were calculated for each C-fragment according to eq 1. For the S461L C-fragment, two trials yielded values of 1.9 ± 0.4 and 2.0 ± 0.6 which confirmed that the high-molecular mass form of S461L was dimeric. The ratio of the S325L C-fragment was determined in four separate trials and yielded 3.1 ± 0.6, 3.1 ± 0.4, 3.1 ± 0.4, and 3.3 ± 0.5, providing evidence that the high-molecular mass species of the S325L C-fragment was a trimer. Further evidence for the trimeric arrangement of subunits in the S325L C-fragment was obtained from an analysis of the equilibrium distribution of monomer and oligomer forms as a function of the total C-fragment concentration. Figure 2 compares the experimental data (●) to the predicted monomer−oligomer equilibria in which the oligomer is either a dimer (---), or a trimer (—). The agreement between the data (slope = 2.8) and the concentration dependence predicted for a trimer support the conclusion that the high-molecular mass form observed in the GFC traces of the S325L C-fragment is a trimer. It is probable that in the association−dissociation process of the S325L

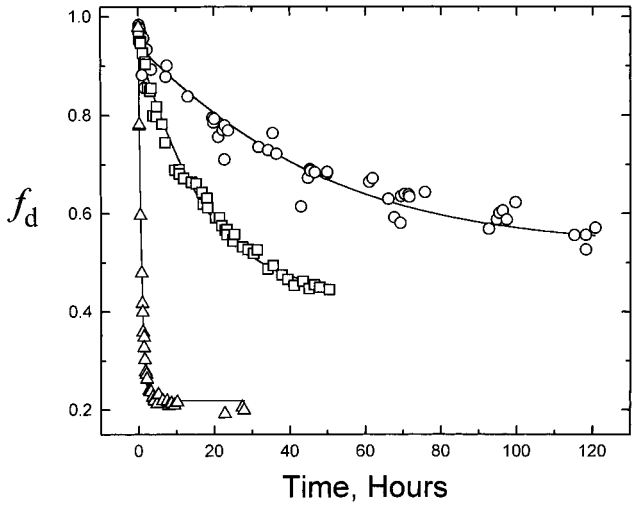

FIGURE 3: GFC kinetic data for the S461L C-fragment protein at three temperatures. The fraction of dimer is plotted as a function of time for a 2.9 μM sample at 4.0 °C (○), a 4.0 μM sample at 14.0 °C (□), and a 3.1 μM sample at 30.0 °C (△). Curves are fits of the data to eq 3.

C-fragment a dimeric intermediate is present. A species which may be this dimeric form is sometimes observed in small amounts (<10%) in the GFC traces of S325L and has an elution volume between that of the monomer and trimer (Long & Weis, 1992). Due to its small contribution to the total protein in the sample, the clustering process for the S325L C-fragment was treated in the simplest terms compatible with the data, as an overall monomer−trimer process without considering intermediates.

C-Fragment Oligomers Dissociate Slowly. The rates of oligomer dissociation for the S461L and S325L C-fragments were studied by collecting the GFC fractions containing the C-fragment in the oligomeric form at 4 °C and then measuring the rate of oligomer dissociation at various temperatures (4.0−30.0 °C), until equilibrium was re-established in the diluted samples. The dimer fractions (f_d) of the S461L C-fragment at 4.0, 14.0, and 30.0 °C are plotted in Figure 3, in which the symbols depict the experimental data and the curves are the fits of the data to the integrated rate equation (eq 3) for the dissociation of a dimer. From these data, it can be seen that both the dissociation rate and the equilibrium level of dissociation are sensitive functions of temperature. The strong temperature dependence of the dissociation process is reflected in the half-lives ($t_{1/2}$) of dimer dissociation at 4.0, 14.0, and 30.0 °C, which were estimated as 85 h, 25 h, and 35 min, respectively (calculated from values of k_d listed in Table 1).

Figure 4 illustrates the difference in the dissociation of the S461L and S325L C-fragments at 14.0 °C. The symbols are experimental data, and the curves are fits of the data to the rate equations for dimer and trimer dissociation, respectively. It can be seen that the rate of dissociation of the S325L C-fragment is larger than that of the S461L protein. The value for $t_{1/2}$ of the S325L oligomer dissociation at 14.0 °C is 4 h, ca. $^1/_6$ of the value of $t_{1/2}$ for the S461L dimer at the same temperature. Since the transition state is likely to resemble the unfolded form of the protein (see below), the lower rate of dissociation of the S461L C-fragment dimer relative to that of the S325L C-fragment trimer is probably a reflection of the greater stability of the S461L C-fragment dimer relative to its denatured state (Wu et al., 1995).

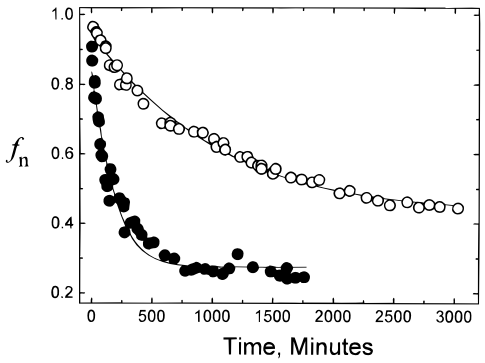

FIGURE 4: Comparison of GFC dissociation data for the S461L and S325L C-fragments. The fraction of oligomer is plotted as a function of time in minutes at 14.0 °C for a 4.0 μM solution of the S461L fragment (○) and a 3.2 μM solution of the S325L fragment (●). Curves are fits of the data to the appropriate rate equations for dissociation of a dimer and a trimer.

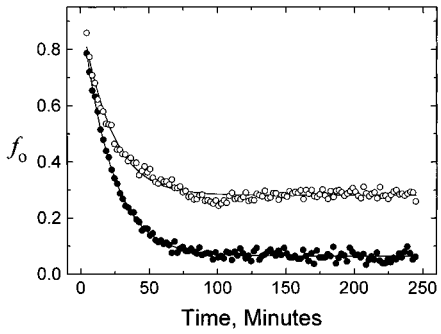

FIGURE 5: Comparison of CD kinetic data for S461L *versus* S325L smooth mutant C-fragments. The fraction of oligomer is plotted as a function of time in minutes for a 6.0 μM sample of the S461L fragment (○) at 30.0 °C and for a 7.9 μM sample of the S325L fragment (●) at 30.0 °C. Curves are fits of the data to the appropriate rate equations for dissociation of a dimer and a trimer.

In addition to GFC, the ellipticity of the C-fragments at 222 nm was used to monitor the dissociation rate of the C-fragment at 23.0 and 30.0 °C. $[\theta]_{222}$ was collected and converted into the fraction of oligomer as described in Materials and Methods. The data obtained at 30.0 °C are plotted as a function of time in Figure 5. Fits of the data were performed to determine k_a, k_d, and K_d. Tables 1 and 2 summarize the calculated kinetic constants obtained for the S461L and S325L C-fragments at all the experimental temperatures. The calculated values of the rate constants from the GFC and CD experiments are in fairly good agreement with each other (Table 1, compare experiments 5 and 6, 8 and 9, 14 and 15, 17 and 18). For the S325L C-fragment, k_a should be regarded as an apparent rate constant (k_{app}), due to the probable existence of intermediates in the association process.

The data clearly demonstrate the slow nature of the C-fragment association−dissociation process. For comparison, the human growth hormone (hGH) displays a monomer−dimer equilibrium with k_a, k_d, and K_d equal to 1.6×10^4 M^{-1} s)$^{-1}$, 2.1×10^{-2} s^{-1}, and 1.3 μM, respectively, at 25 °C (Patapoff et al., 1993). The S461L C-fragment monomer−dimer equilibrium at 23 °C has a comparable value for K_d (10 μM), yet k_a (4 M^{-1} s^{-1}) and k_d (44×10^{-6} s^{-1}) are ca. 10^3−10^4 times smaller than the corresponding constants for hGH dimer dissociation. To cite a second example, the diptheria toxin has been isolated in an inactive dimeric form which slowly converts to the active monomer (~5% dis-

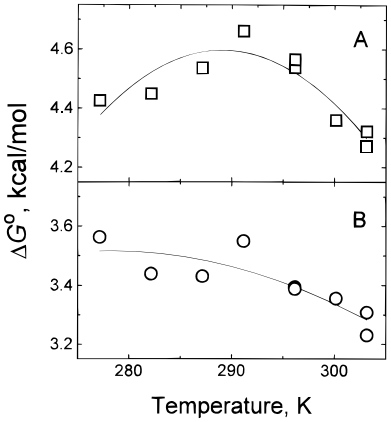

FIGURE 6: $\Delta G°$ values of the oligomer dissociation equilibrium are plotted as a function of temperature for the S325L (A) and S461L (B) C-fragments and are the changes in free energy per mole of monomer. The data were fit to the form for $\Delta G°$ which accounts for the temperature dependence of $\Delta H°$ and $\Delta S°$ (eq 4).

sociation/day at 37 °C; Carroll et al., 1986). The crystal structures of both forms have proven that this interconversion occurs by "domain swapping" (Bennett et al., 1994). As discussed below, the interconversion of the C-fragment between monomer and oligomer shares some of the properties of domain swapping (see the Discussion).

Kinetic studies of leucine zipper peptides have provided estimates for the association and dissociation rates for the reversible dissociation and unfolding process of these dimeric coiled coils ($D_F \rightleftarrows 2M_U$) (Wendt et al., 1995; Zitzewitz et al., 1995), which occurred 10^3-10^4 times more rapidly than the corresponding process for the C-fragment protein. The relatively slow rate of dissociation for the C-fragment may be attributed to the greater length of the putative coiled-coil segment in the C-fragment protein (ca. 60 residues per monomer, see the Discussion) *versus* the leucine zipper coiled coils (23 and 33 residues, respectively), although sequence specific effects on the intrinsic stability of the coiled coils are certain to contribute as well. The difference in the association rates may stem from the fact that the association of the C-fragment probably requires (as described below) associating monomers to unfold significantly before forming an oligomer. In this respect, C-fragment oligomerization resembles a subunit exchange process, whereas the monomeric model peptides are already unfolded to a significant extent. The absence of significant subunit exchange after 16 h at 4 °C between dimers of the yeast transcription activator GCN4 (which form intersubunit contacts via a C-terminal 33-residue coiled-coil domain) is consistent with this view (Hope & Struhl, 1987).

C-Fragment Monomers Are Partially Unfolded. van't Hoff analyses of the S461L and S325L C-fragments equilibria are plotted in Figure 6. Nonlinear least-squares fits of the data yielded the thermodynamic quantities of dissociation for both of the mutants at T_r (298 K) and are listed in Table 3. Positive values of all the parameters ($\Delta H°$, $\Delta S°$, and $\Delta C_p°$) suggest that the monomeric proteins are partly unfolded, in agreement with previous findings (Wu et al., 1995). The increase in heat capacity that is observed when proteins unfold has been attributed to an increase in the exposure of hydrophobic groups to solvent (Brandts, 1964; Sturtevant, 1977; Privalov, 1979; Haynie & Freire, 1993), and thus, the positive values of $\Delta C_p°$ observed for the C-fragment dissociation might also signal an increase in the exposure of hydrophobic groups in the monomer. This effect would appear to be larger for the S325L C-fragment since the $\Delta G°$ of dissociation for this fragment decreases below 290 K, which represents a shift in the equilibrium toward the monomer. This behavior is compatible with the interpretation that more hydrophobic groups are exposed to solvent in the monomer form since a group additivity analysis of amino acid side chain solvation has shown that hydrophobic group exposure becomes less unfavorable thermodynamically at low temperatures relative to the situation at high temperatures (Murphy & Freire, 1992).

Table 3: Thermodynamic Quantities for the C-Fragment Clustering Equilibria[a]

C-fragment	$\Delta G°$ (kcal/mol)	$\Delta H°$ (kcal/mol)	$\Delta S°$ (cal mol^{-1} deg^{-1})	$\Delta C_p°$ (kcal mol^{-1} deg^{-1})
S461L	3.4	7.8	14.7	0.21
S325L	4.4	12.5	27.0	0.89

[a] Values were determined at $T = 298$ K and per mole of monomer.

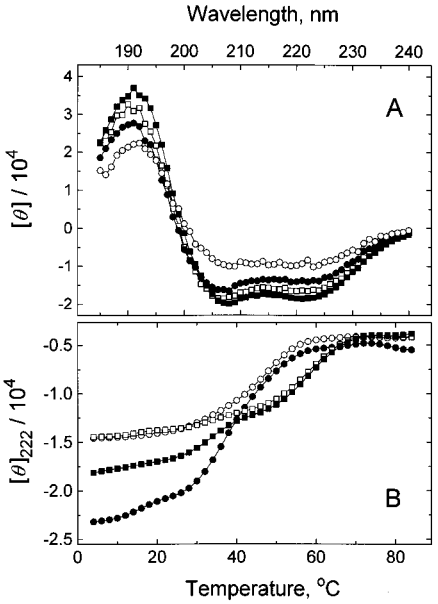

FIGURE 7: CD of the monomer and oligomeric forms of the C-fragments. (A) Far-UV wavelength scans: S461L C-fragment enriched in dimer (■, 83% dimer) and enriched in monomer (□, 85% monomer) and S325L C-fragment samples enriched in trimer (●, 51% trimer) and monomer (○, 93% monomer). (B) Thermal denaturation plots at 222 nm: S461L C-fragment enriched in dimer (■, 95% dimer) and enriched in monomer (□, 97% monomer) and S325L C-fragment samples enriched in trimer (●, 77% trimer) and monomer (○, 94% monomer). The percentages of monomer, dimer, and trimer were determined by GFC.

CD was used to estimate the helix content of the monomer and oligomer forms of the C-fragment proteins. The CD spectra of the S461L (squares) and S325L C-fragments (circles) in Figure 7A demonstrated that samples enriched in the clustered forms of the C-fragments (closed symbols) contained more helical structure than samples enriched in the monomeric form (open symbols). The thermal denaturation curves plotted in Figure 7B also demonstrated the existence of additional helical structure in the clustered forms of the C-fragments. A single transition, corresponding to the main unfolding transition, was observed for samples enriched in the monomeric form of the C-fragment, at 58 °C for a S461L sample that was estimated to be 97% monomer by GFC (□) and at 48 °C for a S325L sample that

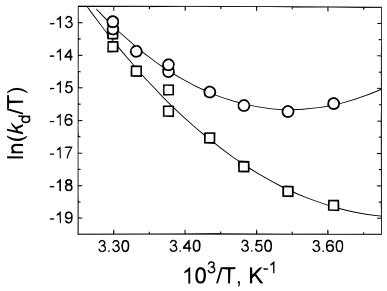

FIGURE 8: Eyring plot of the dissociation kinetics for the S461L (□) and S325L (○) C-fragments. Curves are fits of the data to the temperature-dependent function $\ln(k_d/T)$ (eq 5). The uncertainty in the values of k_d (Tables 1 and 2) produced error bars that were smaller than the width of the data points.

was estimated to be 94% monomer (○). An additional low-temperature transition was observed in C-fragment samples enriched in the clustered form, which was attributed to oligomer dissociation. Apparent values of the transition temperature for dissociation (T_{diss}) were estimated from the derivative of a difference trace obtained by subtracting the thermal denaturation curve of the monomer form from the corresponding curve of a sample enriched in the clustered form (not shown). T_{diss} of the S325L trimer was estimated to be 37 °C in a sample consisting of 77% trimer (●), and for a sample consisting of 95% S461L C-fragment dimer (■), T_{diss} was estimated to be 35 °C. These values of T_{diss} are in good agreement with values from a previous study using samples in which the extent of oligomer formation had not been quantified **(**Wu et al., 1995). It should be noted that T_{diss} has no thermodynamic significance, since the dissociation process is strongly temperature-dependent and thus the values of T_{diss} are expected to be dependent on the scan rate.

Using the estimates of oligomer content for the samples analyzed by CD in Figure 7B, the differences in helix content between the monomer and clustered forms of the C-fragments were approximated using the mean residue ellipticity at 222 nm (in which 100% helix was assumed to have a $[\theta]_{222}$ of $-37\,500$ deg cm^2 dmol^{-1}; Greenfield & Fasman, 1969). The percent α-helix values for the isolated monomer and dimer forms of the S461L C-fragment were estimated to be approximately 38 and 46%, respectively. The S325L C-fragment was found to be approximately 38% helix in its monomer form and 60% helix in its trimer form. These data demonstrated that the monomer forms were significantly less α-helical than the oligomers and provided additional evidence that the monomers were less well-folded than the oligomeric forms.

The Dissociation Transition State Is Significantly Unfolded. Eyring plots of the rate data [$\ln(k_d/T)$ *versus* $1/T$] were used to estimate the thermodynamic parameters of the transition state relative to the clustered state (Figure 8). These data were distinctly nonlinear and thus were fit with a function that accounted for the temperature dependence of $\Delta H^{\circ\ddagger}$ and $\Delta S^{\circ\ddagger}$ through a constant, non-zero value for $\Delta C_p^{\circ\ddagger}$ (eqs 4 and 5). The parameter values which produced the best fit to the data were used to calculate the thermodynamic quantities at 298 K for the transition state of unfolding for both of the mutants, which are listed in Table 4.

Estimates of $\Delta H^{\circ\ddagger}$ for the S325L and S461L C-fragments were calculated at their respective denaturation transition temperatures (ca. 50 and 60 °C; Figure 7B) for the purpose of comparing these values with calorimetrically determined values (ΔH_{cal}) obtained in a study of C-fragment thermal stability (Wu et al., 1995). The magnitudes of the transition state enthalpies at these temperatures are 28 and 50 kcal/(mol of monomer) for the S325L and S461L C-fragments, respectively. Per mole of monomer, these values are comparable (∼70−80%) to the calorimetric enthalpies observed previously [38 and 61 kcal/(mol of monomer) for the S325L and S461L, respectively; Wu et al., 1995] and are thus compatible with the conclusion that, in the transition state, the C-fragments are denatured to a substantial extent. Also, the magnitude of $\Delta S^{\circ\ddagger}$ suggests an increase in the number of configurations of these proteins in the transition state. Finally, the value of $\Delta C_p^{\circ\ddagger}$ [0.7 kcal deg^{-1} (mol of monomer)$^{-1}$, obtained by averaging the two values in Table 4], is comparable to the value of ΔC_p estimated previously by calorimetry [1.0 kcal deg^{-1} (mol of monomer)$^{-1}$; Wu et al., 1995]. Thus, the values of $\Delta H^{\circ\ddagger}$, $\Delta S^{\circ\ddagger}$, and $\Delta C_p^{\circ\ddagger}$ obtained from the analysis using transition state theory suggests that the oligomeric C-fragments unfold significantly during dissociation to the monomeric forms.

Table 4: Thermodynamic Quantities for the Transition State of C-fragment Oligomer Dissociation[a]

C-fragment	$\Delta G^{\circ\ddagger}$ (kcal/mol)	$\Delta H^{\circ\ddagger}$ (kcal/mol)	$\Delta S^{\circ\ddagger}$ (cal/mol deg)	$\Delta C_p^{\circ\ddagger}$ (kcal/mol deg)
S461L	11.2	22.8	26.0	0.77
S325L	7.0	10.7	12.3	0.66

[a] Values were determined at $T = 298$ K and per mole of monomer.

The thermodynamic analysis of coiled coil unfolding and dissociation by Thompson et al. (1993) may be used to show that the process which leads to the transition state of C-fragment dissociation is thermodynamically consistent with the unfolding of the putative coiled-coil segments, on the basis of the empirical relationship between changes in heat capacity and changes in the area of solvent accessible surface (Murphy & Freire, 1992). At 100 °C, the enthalpy change is scaled linearly with changes in the area of solvent accessible polar surface. Using an average enthalpy change per residue [1.2 kcal residue^{-1} (mol of monomer)$^{-1}$] determined using the thermodynamic data for the GCN4 leucine zipper coiled coil (Thompson et al., 1993), the number of coiled-coil residues involved in C-fragment dissociation may be estimated. $\Delta H^{\ddagger}$ of dissociation (at 100 °C) for the S325L and S461L C-fragments is 60 and 80 kcal/mol (Table 4), respectively, resulting in estimates of 50 and 65 coiled-coil residues per monomer, respectively. The two methylation regions (MRs) are predicted to adopt this conformation, and each MR consists of approximately 30 residues (Stock et al., 1991; Cochran & Kim, 1996). Thus, the unfolding of coiled coils may represent the major portion of the structure lost during the process leading to the transition state of oligomer dissociation.

The hydrophobic character of the transition state suggested by the large value of $\Delta C_p^{\circ\ddagger}$ prompted us to examine the effect of detergent on the dissociation kinetics of both smooth mutant C-fragments. A detergent concentration of 0.25% w/v OG was used, which corresponds to approximately $^1/_2$ of the CMC (Jackson et al., 1982). The effects of OG on the dissociation rate of the S461L and S325L fragments at 30.0 and 23.0 °C, respectively, are shown in Figure 9, along with the fits of the data. The dissociation rate constants

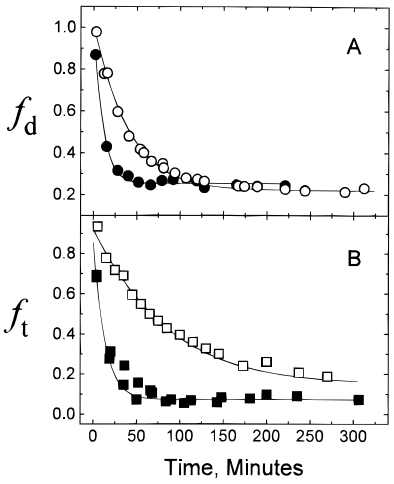

FIGURE 9: GFC kinetic data for the oligomer-forming smooth mutant C-fragment proteins either with or without 0.25% w/v OG. (A) The fraction of dimer is plotted *versus* time for the S461L C-fragment at 30 °C: no OG (○) and 0.25% OG (●). Fits of the data were carried out using eq 3 for dimer dissociation. (B) The fraction of trimer is plotted as a function of time for the S325L C-fragment at 23 °C: no OG (□) and 0.25% OG (■). Fits of the data were determined for a monomer−trimer process using numerical methods as described in Materials and Methods.

determined in the presence of OG (Table 5) increased in the presence of OG 3−5-fold over rate constants determined from samples without OG, suggesting that OG stabilized the transition state via interactions with exposed hydrophobic groups (compare experiments 5 and 8 in Table 1 with 19 and 20 in Table 5 and 14 and 17 in Table 2 with 21 and 22 in Table 5). The amount of stabilization of the transition state is estimated to be 1 kcal/mol for the S461L C-fragment dimer [$\Delta\Delta G^{\circ\ddagger} \approx RT \ln(k_{d,\ 0.25\%\ OG}/k_{d,\ no\ OG})$ at 23 °C]. It may be concluded that OG catalyzes the exchange between monomer and dimer at OG concentrations below the CMC.

DISCUSSION

The most striking features of the data presented in this study are the slow rates of association and dissociation and the strong temperature dependence of the rate process, which provide the evidence that the transition state for the dissociation process resembles unfolded protein. Analysis of the temperature dependence of the dissociation rate by transition state theory has yielded values of $\Delta H^{\circ\ddagger}$ that are approximately 75% of the ΔH_{cal} of unfolding determined calorimetrically. The positive values of $\Delta S^{\circ\ddagger}$ suggest an increase in the number of conformations that are accessible in the transition state, and the positive value of $\Delta C_p^{\circ\ddagger}$, as well as the acceleration of the dissociation reaction by OG, provides evidence of an increase in the exposure of hydrophobic groups to solvent in the transition state. Since the values of all of these parameters are typical of the transition of a protein from a native to an unfolded state, it may be concluded that the transition state for dissociation of the C-fragment oligomers resembles denatured protein.

Coiled-Coil Model for the Dissociation of the C-Fragment. The prediction of a coiled-coil structure for portions of the cytoplasmic domain (Lupas et al., 1991; Cochran & Kim, 1996) and the results of these studies have led us to propose a model for the dissociation of the C-fragment oligomers in which intermolecular coiled coils in the oligomer convert to an intramolecular coiled coil in the monomer (modeled in Figure 10 for the S461L monomer−dimer equilibrium). The two methylation regions, MR1 and MR2, in the cytoplasmic domain contain the methylatable glutamate residues (Kehry & Dahlquist, 1982; Terwilliger & Koshland, 1984) and are predicted to form coiled coils (Lupas et al., 1991; Cochran & Kim, 1996). According to the model depicted in Figure 10, dissociation of the dimer involves significant unfolding because the intermolecular coiled coils must dissociate before reassociating in the monomer (Figure 10).

The results of the experiments reported here create a more detailed picture of the properties of the C-fragments when they are combined with the results of previous studies from our laboratories (Long & Weis, 1992; Wu et al., 1995; Seeley et al., 1996). On the one hand, both monomer and dimer C-fragment proteins are judged to be globally dynamic. This unexpected finding is based on the rapid ($t_{exch} < 15$ min) and extensive (90%) proton exchange rates observed in D_2O labeling experiments (Seeley et al., 1996). Nevertheless, the slow interconversion between monomer and oligomer described in this study indicates that the C-fragments can make long-lived tertiary and quaternary contacts. If the proposed mechanism for dimer dissociation is correct, these contacts will occur in the predicted coiled-coil regions. The results of D_2O exchange experiments are consistent with this analysis, since the model predicts that a commensurate amount of coiled-coil interface will exist in samples of monomer and dimer, and the exchange experiments demonstrated that the amide backbone protons are protected from exchange in the monomer (wild type) and dimer (S461L) C-fragments to approximately equal extents (10%).

Each of the two C-fragments (S325L and S461L) seems to adopt one of the several possible coiled-coil arrangements in the oligomeric state. In the intact receptor dimer, the cytoplasmic domains near the second transmembrane segment are brought together in a parallel fashion. It is therefore plausible that the S461L C-fragment dimer (as depicted in Figure 10) is organized as a parallel intermolecular coiled coil and that the monomer may exist in a hairpin conformation with an antiparallel intramolecular coiled coil. On the other hand, the proposed C-fragment monomer−oligomer interconversion process shares some of the features of domain swapping [reviewed in Bennett et al. (1995)]. The domain swapping formalism predicts that the arrangement of the coiled coils in the monomer and the dimer are the same, i.e. either both parallel or both antiparallel. An even greater number of arrangements are possible in the S325L C-fragment trimer. One arrangement consistent with domain swapping predicts three antiparallel intermolecular coiled-coils contacts in the trimer and an antiparallel coiled coil in the monomer. However, the observation of a relatively large change in the helical content of the S325L trimer relative to that of the monomer is not expected in a domain swapping mechanism, since the interacting structural domains in the monomer and the oligomer are expected to remain essentially unaltered (Bennett et al., 1995). Conformational transitions [e.g. the coiled coil ↔ four-helix bundle transition proposed by Stock and co-workers (1991)] are expected to play a role in the transmembrane-signaling process mediated by these chemoreceptors. In this regard, it might be expected that the monomer−oligomer transitions may partially reproduce these conformational transitions since the mutations were selected on the basis that they appear to lock the receptor into one signaling state and indicates that the mutations

Table 5: Kinetic Data for the S461L and S325L C-Fragments in the Presence of 0.25% OG

no.	C-fragment (concentration, μM)	T (°C)	$f_{n,eq}$	K_d	$k_d \times 10^6$ (s^{-1})	k_a
19	S461L (2.4)	23	0.43 ± 0.01	3.6 μM	220 ± 40	59 ± 10 M^{-1} s^{-1}
20	S461L (2.9)	30	0.25 ± 0.01	13 μM	1010 ± 70	79 ± 6 M^{-1} s^{-1}
21	S325L (2.2)	23	0.08 ± 0.01	150 μM^2	900 ± 300	(6 ± 3) × 10^{-6} M^{-2} s^{-1}
22	S325L (3.5)	30	0.03 ± 0.01	1080 μM^2	1700 ± 700	(2 ± 4) × 10^{-6} M^{-2} s^{-1}

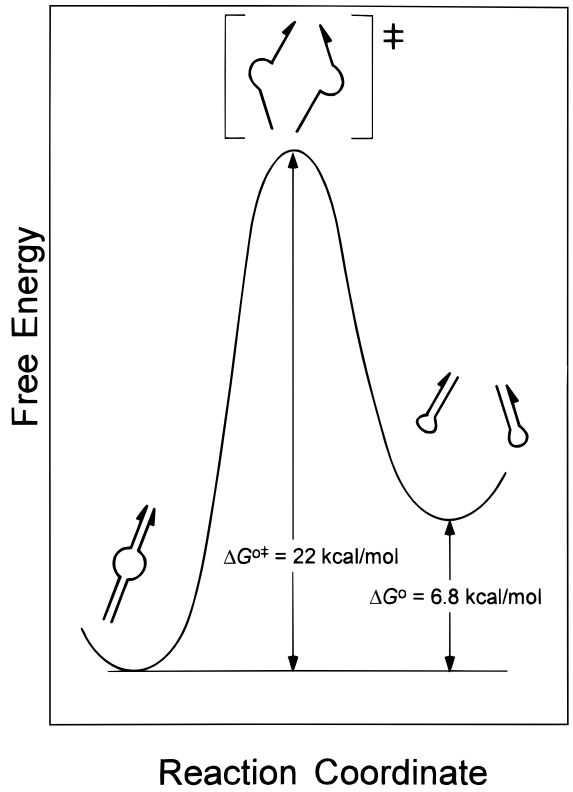

FIGURE 10: Coiled-coil model for the dissociation of the S461L dimeric smooth mutant C-fragment. The dimer (intermolecular coiled coils) is unfolded in the transition state before proceeding to the dissociated monomer state (intramolecular coiled coil). The values of $\Delta G°$ and $\Delta G°^{‡}$ are per mole of dimer at 298 K.

stabilize one conformation relative to the other.

The oligomeric state of the C-fragment is undoubtedly influenced by the nature and the position of the mutation, which is to be expected given the fact that the GCN4 leucine zipper protein can be made to produce two-, three-, or four-helix coiled-coil structures through mutations at positions *a* and *d* of the heptad repeat, which reside at the coiled-coil interface (Harbury et al., 1993). This study also explained the preference for either dimeric or trimeric coiled coils in terms of the packing geometry of amino acids at these interface positions, which concluded that trimeric coiled coils can be thought of as the default oligomerization state. Position 325 is at the end of MR1 in one of the coiled-coil regions and probably corresponds to the *a* position of the heptad repeat (Cochran & Kim, 1996). Thus, the change in hydrophobicity of the serine to leucine mutation may stabilize a three-stranded coiled coil for the S325L C-fragment.

Functional Significance of the Slow Dissociation of the C-Fragment Oligomers. Ligand-induced clustering may be part of the transmembrane-signaling process, although the complete dissociation of intact receptor dimers seems less likely since disulfide-cross-linked receptors are functional (Chervitz et al., 1995; Lee et al., 1995). Nevertheless, changes in receptor subunit contacts may take place during signaling in view of the correlation between the phenotypes of the locked mutants and their tendency to form oligomers (Long & Weis, 1992). There is also growing evidence of a role for receptor subunit interactions which extend beyond the dimer (Maddock & Shapiro, 1993; Cochran & Kim, 1996; Ames et al., 1996; Wu et al., 1996) that has been defined by X-ray crystallography (Milburn et al., 1991), including the observation of interdimer methylation (J. Li, G. Li, and R. M. Weis, unpublished results). Although the C-fragment monomer−oligomer process described in this study may resemble the putative intersubunit rearrangements *in vivo*, the kinetics of rearrangement under physiological conditions will need to occur much more rapidly if they are to be involved in either the excitation or adaptation processes of signal transduction (which have time scales of 200 ms and ~1 s, respectively; Segall et al., 1982, 1986). Subunit rearrangements may occur more quickly in the intact receptor since the orientation of the coiled-coil partners are constrained by their connectivity to the membrane. It can also be speculated that the cytoplasmic-signaling proteins (e.g. CheW) may reduce the barrier to interconversion substantially so that the clustering processes and conformational transitions that are observed for the C-fragment can occur within the appropriate time frame in the intact receptor.

ACKNOWLEDGMENT

The authors thank Dr. John F. Brandts for his helpful discussions and critical reading of the manuscript. We also thank Dr. John V. Seeley for assistance with curve fitting of the monomer−trimer process and Dr. Jamie E. Godfrey for his help in obtaining the light scattering data.

APPENDIX

Derivation of Rate Equations. $f_n(t)$ was determined from the differential equation for the change in the fraction of oligomer as a function of time

$$\frac{df_n}{dt} = -k_d f_n + nk_a M_{tot}^{n-1}(1 - f_n)^n \qquad \text{(A1)}$$

Using the equilibrium condition ($df_n/dt = 0$), $nk_a M_{tot}^{n-1}$ could be eliminated from eq A1 by the equality

$$nk_a M_{tot}^{n-1} = \frac{k_d f_{n,eq}}{(1 - f_{n,eq})^n} \qquad \text{(A2)}$$

which results in the general equation

$$\frac{df_n}{f_{n,eq}(1 - f_n)^n/(1 - f_{n,eq})^n - f_n} = k_d\, dt \qquad \text{(A3)}$$

in which the variables have been separated. In the case of

a dimer ($n = 2$), the equation may be integrated directly either by the method of partial fractions or by a resort to formulae [e.g. Gradshsteyn and Ryzhik (1980)] to give

$$\ln\left(\frac{f_d - 1/f_{d,eq}}{f_d - f_{d,eq}}\right) = \left(\frac{1 + f_{d,eq}}{1 - f_{d,eq}}\right)k_d t + C \qquad \text{(A4)}$$

in which f_d is the fraction of dimer at time t, $f_{d,eq}$ is the fraction of dimer at equilibrium and C is the constant of integration. Application of the initial condition $f_d(0) = f_{d,0}$ leads to eq 3 in the text. In the case of $n = 3$, numerical methods were used to evaluate the differential equation (eq A3) as described in Materials and Methods.

REFERENCES

Ames, P., & Parkinson, J. S. (1988) *Cell 55*, 817−826.
Ames, P., Yu, Y. A., & Parkinson, J. S. (1996) *Mol. Microbiol. 19*, 737−745.
Angelides, K. J., Akiyama, S. K., & Hammes, G. G. (1979) *Proc. Natl. Acad. Sci. U.S.A. 76*, 3279−3283.
Bennett, M. J., Choe, S., & Eisenberg, D. (1994) *Proc. Natl. Acad. Sci. U.S.A. 91*, 3127−3131.
Bennett, M. J., Schlunegger, M. P., & Eisenberg, D. (1995) *Protein Sci. 4*, 2455−2468.
Blair, D. F. (1995) *Annu. Rev. Microbiol. 48*, 489−522.
Bowie, J. U., Pakula, A. A., & Simon, M. I. (1995) *Acta Crystallogr. D51*, 145−154.
Brandts, J. F. (1964) *J. Am. Chem. Soc. 86*, 4302−4314.
Carroll, S. F., Barbieri, J. T., & Collier, R. J. (1986) *Biochemistry 25*, 2425−2430.
Chervitz, S. A., Lin, C. M., & Falke, J. J. (1995) *Biochemistry 34*, 9722−9733.
Cochran, A. G., & Kim, P. S. (1996) *Science 271*, 1113−1116.
Dollinger, G., Cunico, B., Kunitani, M., Johnson, D., & Jones, R. (1992) *J. Chromatogr. 592*, 215−228.
Glasstone, S., Laidler, K. J., & Eyring, H. (1941) in *The Theory of Rate Processes*, pp 442−447, McGraw-Hill Book Co., New York.
Gradshsteyn, I. S., & Ryzhik, I. M. (1980) in *Tables of Integrals, Series, and Products*, p 68, Academic Press, New York.
Greenfield, N., & Fasman, G. D. (1969) *Biochemistry 8*, 4108−4116.
Harbury, P. B., Zhang, T., Kim, P. S., & Alber, T. (1993) *Science 262*, 1401−1407.
Haynie, D. T., & Freire, E. (1993) *Proteins: Struct., Funct., Genet. 16*, 115−140.
Hazelbauer, G. L., Berg, H. C., & Matsumura, P. (1993) *Cell 73*, 15−22.
Hope, I. A., & Struhl, K. (1987) *EMBO J. 6*, 2781−2784.
Jackson, M. L., Schmidt, C. F., Lichtenberg, D., Litman, B. J., & Albert, A. D. (1982) *Biochemistry 21*, 4576−4582.
Kaplan, N., & Simon, M. I. (1988) *J. Bacteriol. 170*, 5134−5140.
Kehry, M. R., & Dahlquist, F. W. (1982) *J. Biol. Chem. 257*, 10378−10386.
Lee, G. F., Burrows, G. G., Lebert, M. R., Dutton, D. P., & Hazelbauer, G. L. (1994) *J. Biol. Chem. 269*, 29920−29927.
Lee, G. F., Lebert, M. R., Lilly, A. A., & Hazelbauer, G. L. (1995) *Proc. Natl. Acad. Sci. U.S.A. 92*, 3391−3395.
Long, D. G., & Weis, R. M. (1992) *Biochemistry 31*, 9904−9911.
Lupas, A. N., Dyke, M. V., & Stock, J. B. (1991) *Science 252*, 1162−1164.
Maddock, J. R., & Shapiro, L. (1993) *Science 259*, 1717−1723.
Milburn, M., Privé, G., Milligan, D. L., Scott, W., Yeh, J., Jancarik, J., Koshland, D. E., Jr., & Kim, S.-H. (1991) *J. Biol. Chem. 254*, 1342−1347.
Milligan, D. L., & Koshland, D. E., Jr. (1988) *J. Biol. Chem. 263*, 6268−6275.
Murphy, K. P., & Freire, E. (1992) *Adv. Protein Chem. 43*, 313−361.
Mutoh, N., Oosawa, K., & Simon, M. I. (1986) *J. Bacteriol. 167*, 992−998.
Oosawa, K., Mutoh, N., & Simon, M. I. (1988) *J. Bacteriol. 170*, 2521−2526.
Pakula, A. A., & Simon, M. I. (1992) *Proc. Natl. Acad. Sci. U.S.A. 89*, 4144−4148.
Parkinson, J. S. (1993) *Cell 73*, 857−871.
Patapoff, T. W., Mrsny, R. J., & Lee, W. A. (1993) *Anal. Biochem. 212*, 71−78.
Press, W. H., Flannery, B. P., Teukolsky, S. A., & Vetterling, W. T. (1986) in *Numerical Recipes. The Art of Scientific Computing*, pp 547−562, Cambridge University Press, New York.
Privalov, P. L. (1979) *Adv. Protein Chem. 33*, 167−241.
Seeley, S. K., Weis, R. M., & Thompson, L. K. (1996) *Biochemistry 35*, 5199−5206.
Segall, J. E., Manson, M. D., & Berg, H. C. (1982) *Nature 296*, 855−857.
Segall, J. E., Block, S. M., & Berg, H. C. (1986) *Proc. Natl. Acad. Sci. U.S.A. 83*, 8987−8991.
Stock, J. B., Lukat, G. S., & Stock, A. M. (1991) *Annu. Rev. Biophys. Biophys. Chem. 20*, 109−136.
Sturtevant, J. M. (1977) *Proc. Natl. Acad. Sci. U.S.A. 74*, 2236−2240.
Terwilliger, T. C., & Koshland, D. E., Jr. (1984) *J. Biol. Chem. 259*, 7719−7725.
Thompson, K. S., Vinson, C. R., & Freire, E. (1993) *Biochemistry 32*, 5491−5496.
Ullrich, A., & Schlessinger, J. (1990) *Cell 61*, 203−212.
Wendt, H., Berger, C., Baici, A., Thomas, R. M., & Bosshard, H. R. (1995) *Biochemistry 34*, 4097−4107.
Wu, J., Long, D. G., & Weis, R. M. (1995) *Biochemistry 34*, 3056−3065.
Wu, J., Li, J., Li, G., Long, D. G., & Weis, R. M. (1996) *Biochemistry 35*, 4984−4993.
Yeh, J. I., Bieman, H.-P., Pandit, J., Koshland, D. E., Jr., & Kim, S.-H. (1993) *J. Biol. Chem. 268*, 9787−9792.
Zitzewitz, J. A., Bilsel, O., Luo, J., Jones, B. E., & Matthews, C. R. (1995) *Biochemistry 34*, 12812−12819.

BI961749I